Modeling the Distribution of the Volcanic Aerosol Cloud from the 1783-1784 Laki Eruption

Luke Oman[1], Alan Robock[1], Georgiy L. Stenchikov[1], Thorvaldur Thordarson[2,3], Dorothy Koch[4,5], Drew T. Shindell[4,5], and Chaochao Gao[1]

[1]*Department of Environmental Sciences, Rutgers University, New Brunswick, New Jersey*
[2]*Department of Geology and Geophysics, University of Hawaii, Honolulu, Hawaii*
[3]*Earth Science Institute, University of Iceland, Reykjavik, Iceland*
[4]*Center for Climate Systems Research, Columbia University, New York*
[5]*NASA Goddard Institute for Space Studies, New York*

Journal of Geophysical Research, in press

November 2005

Revised, January 2006

Corresponding author:
Luke Oman
Department of Environmental Sciences
Rutgers University
14 College Farm Road
New Brunswick, NJ 08901-8551
Phone: 732-932-3891
Fax: 732-932-8644
E-mail: oman@cep.rutgers.edu

Abstract

We conducted simulations of the atmospheric transformation and transport of the emissions of the 1783-1784 Laki basaltic flood lava eruption (64.10°N, 17.15°W) using the NASA Goddard Institute for Space Studies modelE climate model coupled to a sulfur cycle chemistry model. The model simulations successfully reproduced the aerosol clouds of the 1912 Katmai and 1991 Mount Pinatubo eruptions, giving us confidence in the Laki simulations. Simulations of the Laki eruption produce peak zonal mean sulfate (SO_4) concentrations of over 70 ppbv during August and into September 1783 in the upper troposphere and lower stratosphere at high latitudes. While the majority of the sulfate aerosol was removed during the fall and early winter, a significant aerosol perturbation remained into 1784. The peak SO_2 gas loading was just over 37 megatons (Mt) in late June with the sulfate loading peaking in late August 1783 at 60 Mt over the average of 3 runs. This yielded a peak sulfate aerosol (75% H_2SO_4, 25% H_2O) loading of over 80 Mt with the total aerosol produced during the entire eruption of about 165 Mt. The resulting sulfate deposition compares well with ice cores taken across Greenland. The top of atmosphere net radiative forcing peaks at –27 W/m^2 over the high latitudes during late summer 1783 and produces a global mean forcing of –4 W/m^2. The model results confirm that Northern Hemisphere high-latitude volcanic eruptions produce aerosols that remain mostly confined north of 30°N latitude.

1. Introduction

Strong volcanic eruptions that inject large amounts of sulfur dioxide (SO_2) gas into the atmosphere have the ability to significantly perturb our climate system [*Robock*, 2000]. The amount of SO_2 gas, the latitude [*Oman et al*., 2005], and the altitude of the injection all play important parts in the overall climate impact. Recent eruptions like the June 15, 1991 eruption of Mount Pinatubo have had access to satellite [*Long and Stowe*, 1994; *Thomason et al*., 1997] and lidar measurements to construct accurate aerosol cloud data sets [*Stenchikov et al*., 1998; *Antuña et al*., 2003]. Reconstructing the optical depth perturbations from eruptions at the end of the 1800's into the mid 1900's have relied mostly on pyrheliometric data from a number of observing stations [*Sato et al*., 1993; *Stothers*, 1996a; *Stothers*, 1997]. Unfortunately, further back in time less information is available for constructing optical depth data sets. One eruption that is of high interest is the Laki basaltic flood lava eruption that occurred in Iceland (64.10°N, 17.15°W) from June 1783 through February 1784.

The Laki eruption is known locally as the Skaftár Fires [*Thordarson et al.*, 1993] and is one of the largest basaltic lava flows in the last 1000 years. The eruption is sometimes called Lakagígar, which is the name of the cone-row where the fissure eruption occurred. The total volume of magma erupted is estimated at 15.1±1.0 km^3, of which 14.7 km^3 was emplaced as lava and 0.4 km^3 as tephra [*Thordarson et al.*, 1993] and approximately 122 megatons (Mt) of SO_2 gas was released by the eruptions [*Thordarson and Self*, 2003].

Thordarson and Self [2003] produced a complete review of the environmental as well as atmospheric impacts associated with the Laki eruption. Previous studies have constructed estimates of atmospheric SO_2 gas emissions [*Thordarson et al*. 1996], which can be used in conjunction with chemistry and transport models to calculate the atmospheric sulfate loading

resulting from Laki. One such study was conducted by *Stevenson et al*. [2003], in which they used the United Kingdom Met Office 3-D Lagrangian chemistry transport model coupled to the Unified Model general circulation model (GCM). In that study they conducted simulations based on differing assumptions of the vertical distribution of SO_2 gas from the Laki eruption. The simulation of *Stevenson et al*. [2003] deposited 64-72% of the SO_2 gas to the surface before it could react to form sulfate aerosol. The remainder was converted into sulfate aerosol in the model, but it only produced minor climate anomalies [*Highwood and Stevenson*, 2003]. A number of more significant climate anomalies were documented around the Northern Hemisphere (NH) following the Laki eruption [*Thordarson and Self*, 2003; *Stothers*, 1996b], however. The summer of 1783 was very warm in Western Europe with the warmest days often associated with the thick sulfurous dry fog. [*Grattan and Sadler*, 1999; *Thordarson and Self*, 2003]. Alaska and Northwest Canada experienced an extremely cold summer [*Jacoby et al.,* 1999] as did most of Northern Asia, Iceland, and the Faeroe Islands [*Thordarson and Self*, 2003]. The winter of 1783-84 was unusually cold over Europe and the Northeastern United States [*Thordarson and Self*, 2003], with anomalies on the order of –3°C. More recently, *Chenet et al.* [2005] used the LMDZT-INCA model, coupled to an atmospheric chemistry module, to transport 200 Mt of sulfate aerosol estimated from Laki, but did not allow the circulation to react to the radiative forcing from the aerosols. They used a smoothed monthly emission of sulfate aerosol and put 20% at 5 km and 80% at 10 km, which they state is a lower altitude than other studies suggest and is likely an underestimate. *Chenet et al.* [2005] found that the aerosols took about 5 days to reach France from Iceland which is agreement with observations from *de Montredon* [1784].

The volcanic gases and resulting aerosols from the Laki eruption produced severe environmental and health affects [*de Montredon*, 1784; *Grattan*, 1998; *Durand and Grattan*, 1999; *Thordarson and Self*, 2003; *Grattan et al*., 2005]. An estimated 24% of the population of Iceland died as a result of the Laki eruption [*Finnsson*, 1796] and increases in the death rate were seen across Europe [*Grattan et al*., 2005]. The sulfuric acid aerosol cloud that hung over the NH following the Laki fissure eruption was often referred to as a dry fog or haze, which was present in the lower troposphere (LT) until late October 1783 and the upper troposphere/lower stratosphere (UT/LS) until at least February 1784 [*Thordarson and Self*, 2003]. To better understand the climate response, as well as environmental and health effects, an accurate distribution of the volcanic aerosols must be determined. Coupled chemistry/climate models offer a way to examine these issues. We first validate the model by conducting simulations of the sulfate aerosols resulting from more recent volcanic eruptions, for which more information is known.

The goal of this paper is to model the chemical transformation and resulting gas and aerosol distribution from the Laki eruption to create a data set that can be used by modeling groups to better understand the climate response from these aerosols. In section 2 we briefly describe the Goddard Institute for Space Studies (GISS) modelE GCM and the coupled sulfur cycle model. The volcanic SO_2 gas emissions used in our simulations are described in section 3. Section 4 presents the results of our model testing as well as our modeling of the Laki eruption. The radiative impact from an off-line simulation using the Laki data set is described in section 5, with discussion and conclusions in section 6.

2. Model Description

The simulations were conducted using the stratospheric version of the GISS modelE GCM. A complete overview of the model can be found in *Schmidt et al*. [2006]. This particular configuration of the model has a 4° latitude by 5° longitude grid with 23 vertical levels up to 80 km and has a full gravity wave drag scheme. This scheme separately calculates the effects of gravity waves forming from mountain drag, penetrating convection, shear and deformation [*Schmidt et al*., 2006], which leads to better simulation of the stratosphere. The model uses the correlated *k* distribution method radiation scheme from *Lacis and Oinas* [1991]. This method allows implicit representation of absorption and scattering [*Hansen et al*., 2002] over 33 *k* intervals in the thermal spectrum. In addition we used an on-line sulfur chemistry model [*Koch et al.*, 2006], which has prognostic dimethyl sulfide (DMS), SO_2, sulfate (SO_4), and hydrogen peroxide (H_2O_2). We used fixed monthly hydroxyl radical (OH) concentrations from *Jöckel et al*. [2003].

Our estimates of SO_2 gas emission are injected into the atmosphere and are chemically converted by 2 main pathways. In the stratosphere the predominant chemical reaction is the gas phase oxidation of SO_2 gas with OH to form sulfate aerosol. The chemical conversion is described by *Bekki* [1995]:

$$SO_2 + OH + M \rightarrow HSO_3 + M \quad (1)$$

$$HSO_3 + O_2 \rightarrow HO_2 + SO_3 \quad (2)$$

$$SO_3 + H_2O \rightarrow H_2SO_4 \quad (3)$$

In the troposphere SO_2 gas is converted to sulfate aerosol by the gas phase reactions (1-3) as well as by aqueous phase reactions with H_2O_2 [*Koch et al*., 1999]:

$$SO_2(aq) \rightarrow HSO_3^- + H^+ \quad (4)$$

$$HSO_3^- + H_2O_2\,(aq) + H^+ \rightarrow SO_4^{-2} + H_2O + 2H^+ \quad (5)$$

The model calculates the radiative properties of hygroscopic sulfate aerosols, which depend explicitly on the local relative humidity [*Tang*, 1996; *Schmidt et al*., 2006]. The dry deposition module uses a resistance-in-series scheme similar to the one used by *Koch et al.* [1999], except with better coupling to GCM processes [*Koch et al*., 2006]. The model's wet deposition is fully coupled to the GCM's hydrologic cycle, including the convection scheme. Also, the model includes settling of small particles, including situations where the mean free path of air is larger than the particle radius which is important in the stratosphere [*Koch et al*., 2006].

3. Volcanic Data Sets

The data set used in reconstructing the Laki eruption comes from the work of *Thordarson and Self* [2003]. They calculated a total 122 Mt of SO_2 gas released by the Laki flood lava eruption. In our Laki simulation we injected 94.3 Mt of SO_2 during 10 explosive eruption events over a 5 month period into the UT/LS. *Thordarson and Self* [2003] also estimated that lava degassing caused an additional 27.7 Mt of SO_2 to be injected into the LT over an 8 month period. While this is the best estimate we have available of the SO_2 emitted by Laki, there are uncertainties which we estimate to be about ±20%. We simulated this by injecting the UT/LS SO_2 gas into the model around 9-13 km above the grid box covering Iceland with the LT component put in as a daily emission between the surface and 2 km. The uncertainties associated with the altitude of our UT/LS component are likely ±3 km from the center of our injection. The altitude of the SO_2 gas is important in determining the lifetime of the gas as well as the resulting sulfate aerosol, with the lifetime of both increasing with altitude. Figure 1 shows the daily emissions of SO_2 gas (Mt) used in the model for the Laki eruption.

Before we conducted the Laki simulations, we first tested the model's ability to reproduce more recent volcanic aerosol distributions. We used the Mount Pinatubo eruption to see how well the model can reproduce the aerosol distribution following a tropical volcanic eruption. We injected 20 Mt of SO_2 gas [*Bluth et al*., 1997] into the stratosphere mostly between 19 and 29 km over the grid box covering Mount Pinatubo (15°N) on 15 June 1991. Also, we conducted simulations of the high-latitude Katmai eruption (58°N) in which 5 Mt of SO_2 gas was injected between 15 and 24 km [*Stothers*, 1996a] on 6 June 1912. While much less information is available for Katmai it is the most recent high-latitude eruption with significant SO_2 gas emission.

4. Results

Since only a limited amount of information is known about the Laki flood lava eruption, it is best to test the model's ability to reproduce more recent eruptions in which more data have been collected. While the sulfur chemistry model has been thoroughly tested and validated in the troposphere [*Koch et al*., 2006], little has been done in the stratosphere. To see how the model handles large injections of SO_2 gas into the stratosphere we first simulated volcanic eruptions for which much more information is available for validation. The 1991 Mount Pinatubo eruption is the best observed volcanic eruption to date. We conducted three simulations, with different initial conditions, of the Mount Pinatubo eruption to test the e-folding time of transformation of SO_2 gas to sulfate aerosol as well as the transport and removal of the sulfate aerosol. Since Laki was a high-latitude eruption we also conducted three simulations, with different initial conditions, of the 1912 Katmai eruption to compare the response to reconstructed data sets. By conducting three ensemble simulation of each eruption, we can see the impact that meteorology has on the uncertainty of the evolution of the aerosol distribution.

4.1. Model tests with Katmai and Pinatubo

Observational evidence indicates that the e-folding time of SO_2 following the Mount Pinatubo eruption was between 33 and 35 days [*Bluth et al*., 1992; *Read et al*., 1993]. Our model simulations produce an e-folding time of 35 days, which is very good compared to observations. The e-folding time for sulfate aerosol after Pinatubo was found to be in the range of 12-14 months [*Lambert*, 1993; *Baran and Foote*, 1994; *Bluth et al.*, 1997; *Barnes and Hoffman*, 1997]. The model has a sulfate aerosol decay of approximately 13-14 months–just on the high side of observations. In the case of the Katmai eruption no direct observations exist of the e-folding time of SO_2, however the model calculated value is 38 days which is slightly longer than following Mount Pinatubo. One reason is the slightly lower OH concentrations at high latitudes compared to the tropics. *Stothers* [1996a] reports an approximate 9-10 month e-folding time for sulfate aerosols from Katmai. Our model simulation produces a slightly shorter but reasonable e-folding time of 8-9 months. It appears that in high-latitude volcanic eruptions the sulfate aerosol decays slightly faster then after a tropical eruption based on modeling and observational data, which is due in part to the Brewer-Dobson stratospheric overturning circulation [*Holton et al.,* 1995]. This however, will also depend on the height of the stratospheric injection of SO_2 gas.

Figure 2 shows the modeled global atmospheric loading of SO_2 and SO_4 for the three simulations of the Mount Pinatubo and Katmai eruptions. The 20 Mt of SO_2 gas was converted into a peak SO_4 loading of just over 27 Mt about 5 to 6 months after the eruption. Assuming a sulfate aerosol concentration of 75% H_2SO_4 and 25% H_2O this would yield a peak aerosol loading of about 36 Mt. Observational evidence indicates between 21 and 40 Mt of sulfate aerosol was produced [*Russell et al*., 1996]. *Stothers* [1996a] estimated the Katmai eruption

dispersed 5 Mt of SO_2, which was converted into 11 Mt of sulfate aerosol. In the case of modelE, 5 Mt of SO_2 was injected into the stratosphere and ultimately converted into a peak SO_4 loading of almost 7 Mt. If we assume the same aerosol composition as Pinatubo the peak hydrated aerosol loading should be about 9.3 Mt, which is slightly less than estimated from observational data, but comparable to the estimates based on the petrologic method [*Stothers*, 1996a; *Palais and Sigurdsson*, 1989].

In our model simulations we use effective radii that correspond to the individual eruption, based on the work of *Stothers* [2001]. The average hydrated sulfate aerosol effective radii for the Mount Pinatubo eruption used in our study was between 0.45 and 0.52 μm. For the Katmai eruption the effective radii were smaller and in our simulations were between 0.30 and 0.34 μm. Figure 3 shows the zonal mean sulfate visual optical depth from Mount Pinatubo produced by modelE compared to SAGE II [*Thomason et al*., 1997] and AVHRR [*Long and Stowe*, 1994] as well as the global average optical depth for all of these. The model produces a reasonable global average optical depth of 0.14, which is the same as observations from SAGE II although the aerosol peak optical depth is about 3 months earlier in our model simulations. This timing of the peak optical depth coincides better with AVHRR, however the peak value is higher in the AVHRR data. The modeled e-folding time of the sulfate aerosol is very similar to both SAGE II and AVHRR data, which is a little over 1 year. The modeled peak maximum tropical optical depth is just over 0.33, this is in the middle of the range with AVHRR just over 0.43 and SAGE II around 0.22.

One of the clear differences with the modelE simulations is the faster poleward transport of the sulfate aerosol, which is reflected in the optical depth perturbation, and reflects an inability to properly simulate the stratospheric tropical aerosol reservoir [*Grant et al*., 1996]. This is

similar to ECHAM4 simulations of the Mount Pinatubo eruption [*Timmreck et al.*, 1999], in which they cite the model's inability to properly simulate the quasi-biennial oscillation (QBO) as one reason for this difference. *Trepte and Hitchman* [1992] showed noticeable differences in the patterns of aerosol transport based on the shear phase of the QBO. *Choi et al*. [1998] found that during the easterly shear phase of the QBO (which was observed during the early months following the Mount Pinatubo eruption), the aerosols experienced an equatorward transport lengthening the lifetime of this tropical maximum. While this causes a noticeable impact on the ultimate aerosol distribution after tropical eruptions, it should have little impact in simulating high-latitude volcanic eruptions, which typically have aerosols confined to the extratropics. ModelE also has trouble simulating the strong latitudinal gradients seen in observations in the vicinity of either the subtropical or polar regions. This is consistent with studies of the age-of-air and the distribution of long-lived trace gases such as CH_4 and N_2O in the stratosphere, both of which show excessive mixing across both the subtropical and polar semi-permeable transport barriers in this version of the model [*Shindell et al*., manuscript in preparation].

Figure 4 shows the zonal mean sulfate optical depth for the Katmai eruption from our modelE simulations, *Ammann et al*. [2003] and *Sato et al*. [1993] observations, and the NH average optical depth for all of these. Observations indicate that high-latitude volcanic eruptions like Katmai typically have aerosols that remain in the hemisphere in which they are injected with the majority remaining north of 30°N latitude for a NH high-latitude eruption [*Lamb*, 1970]. Our model simulations of the Katmai eruption confirms this observation, with only a small amount of aerosol south of 30°N latitude.

The NH average optical depth for modelE is just under 0.1, compared to 0.15 for Ammann and 0.08 for Sato. The e-folding time of our simulations is about 8-9 months, a slightly

faster decay than the Mount Pinatubo simulation. Ammann uses an estimate of 1 year for all eruptions, both tropical and high-latitude. The e-folding time of the Sato data set is almost 2 years, which is much higher than the time reported by *Stothers* [1996a] of 9-10 months based on pyrheliometric observations following the eruption. The Sato data set includes 2 much smaller volcanic eruptions following Katmai which are not included in Ammann or our modelE results and causes this much higher e-folding time. The peak optical depth for the model simulation is about 0.27, which is slightly less than the 0.3 from Ammann but significantly more than Sato's 0.12. The timing of the peak optical depth is similar for all three with Sato and Ammann in August and modelE one month later in September. Based on this information it appears that modelE can reasonably simulate the chemical conversion and transport of a high-latitude volcanic eruption.

4.2. Laki simulations

Since the model is able to reasonably reproduce these relatively well-observed eruptions, we next conducted three simulations of the Laki eruption based on the estimated atmospheric inputs of *Thordarson and Self* [2003]. The daily SO_2 and SO_4 mass loadings are shown in Figure 5 for the Laki eruption. A peak of just over 37 Mt of SO_2 occurs in late June following three very large eruption episodes. The model produces a peak in SO_4 in late August between 55 and 64 Mt, which is equivalent to just over 80 Mt of sulfate aerosol on average (assuming the same composition as after Pinatubo). The e-folding time of the sulfate aerosol is approximately 4 months. This shorter e-folding time is due to the much lower height of the sulfate aerosol compared to the Katmai eruption. While the bulk of this aerosol is removed during the fall and early winter of 1783 a significant loading is still visible into 1784. Since very little information is known about the effective radii resulting from the Laki eruption, an estimate must be used to

evaluate the optical depth and the radiative forcing from the eruption. *Pinto et al.* [1989] used a microphysical model to evaluate the resulting mode radii produced by different sized eruptions. Based on their study we estimate that Laki should have effective radii about 20% larger than Mount Pinatubo in the UT/LS. In our simulations the average UT/LS effective radius is between 0.54 and 0.61 μm. Figure 6 shows the calculated zonal mean sulfate optical depth for the three Laki runs as well as the NH average optical depth. The optical depth perturbations are very similar for the three runs with maximum values of between 1.4 and 2 over the highest latitudes during August and into September. The peak NH average optical depth of around 0.5 occurs at the same time and is reduced to 0.1 by January 1784. Most of the aerosols have been removed by July 1784.

Table 1 shows the total sulfate aerosol mass formed in our Laki simulations compared to some past estimates. We assume a 75% H_2SO_4 and 25% H_2O composition for comparison with past studies as this is the typically accepted composition for volcanic aerosols. It is likely, however that the aerosols produced by Laki had a larger percentage of H_2O since the aerosols were lower in height in areas of higher relative humidity. Our model estimates of 163-166 Mt of sulfate aerosol are close to the middle range of estimates from other studies. Estimates based on ice core data range from 46-59 Mt [*Zielinski*, 1995], to 138-210 Mt [*Clausen et al*., 1997], and up to 374 Mt [*Clausen and Hammer*, 1988], although the latter 2 studies were based on nuclear tests assuming mid-stratospheric transport of sulfate aerosols. Estimates based on optical depth calculations produce approximately 200 Mt of aerosol [*Stothers*, 1996b]. Geological estimates from *Thordarson and Self* [2003] also report a total aerosol mass of 200 Mt. The modeling study of *Stevenson et al*. [2003] calculates a range of 71 to 92 Mt depending on the emissions profile used.

One way in which our model estimates can be validated is by comparing sulfate deposition from ice cores in Greenland. The model simulations deposit a range of between 165 to over 300 kg/km^2 over interior Greenland (Figure 7a) with much higher values over the low lying coastal areas. *Clausen and Hammer* [1988] found an average deposition of 168 kg/km^2 in 11 cores, with a range of 62 to 294 kg/km^2. *Mosley-Thompson et al*. [2002] found an average deposition of 175 kg/km^2 in six Program for Arctic Regional Climate Assessment (PARCA) cores with a range of 80 to 324 kg/km^2. The model results seem reasonable compared to these ice core measurements, although the modeled deposition rates over the southern tip of Greenland are larger than observations. Figure 7b shows ice core deposition from a total of 23 Greenland ice cores for comparison [*Gao et al.*, manuscript in preparation].

There has been some debate as to the timing of the Laki sulfate deposition peak in ice cores retrieved from Greenland. *Fiacco et al*. [1994] place the peak in 1784 whereas, others [*Clausen et al*., 1997; *Mosley-Thompson et al.*, 2002] show the peak deposition to be in 1783. Our modeling study shows the majority of deposition to Greenland occurs in 1783. *Fiacco et al*. [1994] used chemical markers, such as chlorine/sodium ratio which has been shown to peak in summer [*Legrand and Delmas*, 1988], to suggest that the deposition of sulfate occurred 1 yr following the deposition of volcanic glass shards from Laki. However, it is possible that since Laki emitted 3.6 Mt of HCl into the UT/LS [*Thordarson et al*., 1996] this chlorine/sodium peak is significantly enhanced by deposition of volcanogenic Cl from the eruption. It would helpful to examine these data in more detail, and data from other ice cores, to see what portion is non-sea-salt chlorine due to Laki.

Figure 8 shows the summer (JJA) average mean SO_2 and SO_4 in ppbv over the longitudes around Europe (averaged from 30°W to 45°E). The peak SO_2 concentrations are just over 70

ppbv over the high-latitude UT/LS. A secondary maximum occurs in the LT between 60 and 70°N latitude of 10 ppbv. The much slower e-folding time of SO_2 in the UT/LS is evident by the much larger horizontal and vertical spreading of the gas. SO_4 concentrations peak in the UT/LS at over 20 ppbv and at around 5 ppbv in the LT high latitudes. While the 30-60°N latitude bands near the surface average between 1-2 ppbv, larger aerosol levels are seen throughout Europe averaging 5-10 ppbv.

The evolution of the zonal mean SO_4 concentration in ppbv is shown in Figure 9 for the Laki eruption at 3 levels. The bottom panel shows the 945 mb level and represents the LT. The peak concentration occurs during the late summer and into early fall at just over 2 ppbv and decreases rapidly once the eruption stops. The center panel shows the concentrations at 280 mb and represents the UT. The concentrations are much higher, peaking above 70 ppbv by August into September. Also, the longer e-folding time is evident as the aerosol is present well into the second summer. The top panel shows the concentrations at 171 mb and represents the LS at high latitudes. A similar peak of over 70 ppbv occurs with a slightly longer e-folding time as would be expected in the LS. Overall, the aerosols are mainly confined north of 30°N latitude although there is some transport south of this latitude.

5. Radiative Impact

Offline calculations of the instantaneous top of atmosphere (TOA) radiative forcing of the Laki eruption were conducted based on the average of the three simulations. The top panel of Figure 10 shows the zonal mean shortwave forcing peaks at around –35 W/m^2 in August and into September at high latitudes. This decreases rapidly with time and is a function of the decreasing aerosol concentration as well as reduced shortwave radiation during fall and winter over the mid and high latitudes. A negative anomaly continues into 1784 but is smaller in

magnitude. The center panel shows the longwave forcing peaks at around 8 W/m^2 around September at about 60°N latitude. The positive longwave forcing continues for the remainder of 1783 but decreases with time also as the concentration decreases. The bottom panel shows the net radiative forcing is around –27 W/m^2 in August over the high latitudes. Some positive radiative forcing occurs over the polar regions in late fall and into early winter. To put this in perspective, the global TOA net radiative forcing peaks at –4 W/m^2 in August 1783 which compares to –2.5 W/m^2 following Pinatubo [*Kirchner et al.*, 1999]. The surface shortwave forcing is slightly less than at the TOA, while the longwave forcing is much less peaking at 1-2 W/m^2.

The heating rate was also calculated for the Laki eruption and Figure 11 shows the August 1783 and January 1784 anomaly in K/day. Figure 11c shows that the August total heating rate anomaly has 2 main areas of positive heating rates. The first area near the UT/LS is mainly from the longwave heating (0.2 K/day) of the main aerosol cloud as well as some additional contribution from incoming near-IR at the top of the cloud [*Stenchikov et al.*, 1998]. The second area which has a maximum between 5 and 10 mb is heating of ozone by reflected ultraviolet radiation from the increased albedo of the sulfate aerosol layer. There are also two main areas of cooling from the eruption. The first is in the low to mid troposphere at high latitudes and is caused by a decrease in the near-IR, which causes less heating of water vapor. This cooling (–0.1 K/day) effect gets stronger poleward with increasing aerosol concentration but is somewhat compensated by the positive heating of the aerosol by outgoing longwave radiation. The other area of cooling (–0.3 K/day) is in the LS and is mainly due to enhanced longwave cooling from the top of the aerosol layer. In contrast we can look at January 1784, with the much lower aerosol concentrations evident in the reduced heating rate anomalies. There

is very little warming in the total heating rates in Figure 10f with some cooling (–0.1 K/day) still present at high latitudes from the enhanced longwave radiation at the top of the aerosol cloud.

6. Discussion and Conclusions

Using the GISS modelE GCM we created a data set of the aerosols produced by the Laki flood lava eruption based on the SO_2 emission estimates provided by *Thordarson and Self* [2003]. The sulfur cycle model had already been successfully tested in the troposphere [*Koch et al.*, 2006] and was tested in the stratosphere in this paper. The model can reasonably reproduce the optical depth perturbations from the Mount Pinatubo and Katmai eruptions. Also, the e-folding time of SO_2 gas and sulfate aerosol were well reproduced by modelE, although one weakness is the inability of the model to accurately reproduce the stratospheric tropical aerosol reservoir after the Mount Pinatubo eruption. Since this is not a feature seen in high-latitude eruptions, it should have little if any impact on our Laki simulations. A series of three ensemble simulations were conducted for each eruption and only small differences were noted between runs. This indicates that different weather in individual runs plays only a small part in the aerosol evolution.

The Laki basaltic flood lava eruption produced an extremely large sulfate aerosol perturbation to the NH climate system, causing large environmental and health affects. Our modeling simulations help to establish the magnitude as well as distribution of this aerosol so that climate models can use this data in order to understand the climate response to such a large sulfate perturbation.

Modeling of the Laki eruption shows that the maximum aerosol concentration occurs from late August and into September with peak concentrations in the UT/LS of over 70 ppbv. The model calculated zonal mean optical depth peaks at 1.4 to 2 over the highest latitudes. The

NH average optical depth peaks in late summer at just over 0.5. The majority of the Laki aerosols are deposited toward the end of 1783 but a significant amount remains in the UT/LS into early 1784. The deposition to the Greenland ice sheet compares favorably to ice core measurements and represents one method of validation for the Laki eruption. Our modeling simulations produce a total aerosol yield of 163-166 Mt which is in the middle of the range of available estimates. Our model simulations show that most of the deposition to the Greenland ice sheet occurs during 1783, which is in agreement with most ice core measurements. This suggests that it would be helpful to further examine the findings in *Fiacco et al*. [1994] and their dating of the Laki sulfate peak as 1784 in the GISP2 ice core. The peak in chlorine/sodium ratio that they found could be due in part to excess chlorine from Laki. *Clausen et al*. [1997] reported that a chlorine peak was typically found in the nearby GRIP ice core along with sulfate deposition from Icelandic eruptions.

A significant radiative perturbation occurs mainly during the summer and fall following the Laki eruption. The TOA net radiative forcing peaks in August 1783 at around –27 W/m^2 over high latitudes. The Laki and Katmai model simulations confirm that the aerosols from NH high-latitude volcanic eruptions remain mostly confined north of 30°N latitude as was found in observations from Katmai [*Stothers*, 1996a].

By verifying our model against past volcanic eruptions we have more confidence in modeling of the Laki eruption. A deposition of 64-72% of the SO_2 gas to the surface before it could react to form sulfate aerosol was found by *Stevenson et al*. [2003], but our results suggest that only 30-35% was not converted to sulfate. Also, the assumption that 100% of the UT/LS SO_2 is converted to sulfate aerosol in the *Chenet et al*. [2005] study is likely high.

The sulfate aerosol data set created in this study will be used to test the climate response of the Laki eruption, which caused a significant aerosol perturbation to the NH. These data will be made available to other modeling groups who would like to examine the climate response from the Laki eruption.

Acknowledgments. We would like to thank Patrick Jöckel and Christoph Brühl for providing the OH data set used in this study. Also, we would like to thank the reviewers for their helpful comments and suggestions. This work is supported by NSF grant ATM-0313592 and NOAA grant NA03-OAR-4310155. Model development at GISS is supported by NASA climate modeling grants.

References

Ammann, C. M., G. A. Meehl, W. M. Washington, and C. S. Zender (2003), A monthly and latitudinally varying volcanic forcing dataset in simulations of 20th century climate, *Geophys. Res. Lett.*, *30*(12), 1657, doi:10.1029/2003GL016875.

Antuña, J. C., A. Robock, G. Stenchikov, J. Zhou, C. David, J. Barnes, and L. Thomason (2003), Spatial and temporal variability of the stratospheric aerosol cloud produced by the 1991 Mount Pinatubo eruption, *J. Geophys. Res.*, *108*(D20), 4624, doi:10.1029/2003JD003722.

Baran, A. J., and J. S. Foot (1994), A new application of the operational sounder HIRS in determining a climatology of sulfuric acid aerosol from the Pinatubo eruption, *J. Geophys. Res.*, *99*, 25,673-25,679.

Barnes, J. E., and D. J. Hoffman (1997), Lidar measurements of stratospheric aerosol over Mauna Loa Observatory, *Geophys. Res. Lett.*, *24*, 1923-1926.

Bekki, S. (1995), Oxidation of volcanic SO_2: a sink for stratospheric OH and H_2O, *Geophys. Res. Lett.*, *22*, 913-916.

Bluth, G. J. S., S. D. Doiron, A. J. Krueger, L. S. Walter, and C. C. Schnetzler (1992), Global tracking of the SO_2 clouds from the June 1991 Mount Pinatubo eruptions, *Geophys. Res. Lett.*, *19*, 151-154.

Bluth, G. J. S., W. I. Rose, I.E. Sprod, and A. J. Krueger (1997), Stratospheric Loading of Sulfur from Explosive Volcanic Eruptions, *J. Geology.*, *105*, 671-683.

Chenet, A.-L. F. Fluteau, and V. Courtillot (2005), Modelling massive sulphate aerosol pollution, following the large 1783 Laki basaltic eruption, *Earth Plan. Sci. Lett.*, *236*, 721-731.

Choi, W., W. B. Grant, J. H. Park, K.-M. Lee, H. Lee, J. M. Russell III (1998), Role of the quasi-biennial oscillation in the transport of aerosols from the tropical stratospheric reservoir to midlatitudes, *J. Geophys. Res*., *103*, 6,033-6,042.

Clausen, H. B. and C. U. Hammer (1988), The Laki and Tambora eruptions as revealed in Greenland ice cores from 11 locations, *Annals of Glaciology*, *10*, 16-22.

Clausen, H. B., C.U. Hammer, C.S. Hvidberg, D. Dahl-Jensen, J. P. Steffensen, J. Kipfstuhl, and M. Legrand (1997), A comparison of the volcanic records over the past 4000 years from the Greeland Ice Core Project and Dye 3 Greenland ice cores, *J. Geophys. Res*., *102*, 26,707-26,723.

de Montredon, M. M. (1784), Recherches sur l'origine et la nature des vapeurs qui ont régné dans l'atmosphère pendant l'été de 1783, *Mém. Acad. Royale des Sciences*, Paris, 754-773.

Durand, M., and J. Grattan (1999), Extensive respiratory health effects of volcanogenic dry fog in 1783 inferred from European documentary sources. *Env. Geochem. Health*, *21*, 371- 376.

Fiacco, J. J., T. Thordarson, M. S. Germani, S. Self, J. M. Palais, S. Withlow, and P. M. Grootes (1994), Atmospheric aerosol loading and transport due to the 1783-84 Laki eruption in Iceland, interpreted from ash particles and acidity in the GISP2 ice core, *Quat. Res., 42*, 231-240.

Finnsson, H. (1796), Um mannfækkun í Hallærum (Decimation of the population in Iceland due to famines), in *Rit Thess konunglega íslenska lærdómslistafélags*, XIV, pp. 30-226, Copenhagen.

Grant, W. B., E. V. Browell, C. S. Long, L. L Stowe, R. G. Grainger, and A. Lambert (1996), Use of volcanic aerosols to study the tropical stratospheric reservoir, *J. Geophys. Res*., *101*, 3,973-3,988.

Grattan, J. P. (1998), The distal impact of volcanic gases and aerosols in Europe: a review of the 1783 Laki fissure eruption and environmental vulnerability in the late 20th century, *Geological Society*, *Special Publications*, *15*(9), 7-53.

Grattan, J., M. Brayshay, and J. Sadler (1998), Modelling the distal impacts of past volcanic gas emissions: evidence of Europe-wide environmental impacts from gases emitted during the eruption of Italian and Icelandic volcanoes in 1783, *Quaternaire*, *9*(1), 25-35.

Grattan, J., and J. Sadler (1999), Regional warming of the lower atmosphere in wake of volcanic eruptions: The role of the Laki fissure eruption in the hot summer of 1783, in *Volcanoes in the Quaternary*, edited by C. R. Firth and W. J. McGuire, Geol. Soc. London, Spec. Pub., 161, 161-172.

Grattan, J., R. Rabartin, S. Self, T. Thordarson (2005), Volcanic air pollution and mortality in France 1783-1784, *C. R. Geoscience, 337*, 641–651.

Hamill, P., E. J. Jensen, P. B. Russell, and J. J. Bauman (1997), The life cycle of stratospheric aerosol particles, *Bull. Am. Meteorol. Soc.*, *78,* 1395-1410.

Hansen, J., et al. (2002), Climate forcings in Goddard Institute for Space Studies SI2000 simulations, *J. Geophys. Res.*, *107*(D18), 4347, doi:10.1029/2001JD001143.

Highwood, E. J., and D. S. Stevenson (2003), Atmospheric impact of the 1783-1784 Laki eruption: Part II climatic effect of sulphate aerosol, *Atmos. Chem. Phys., 3*, 1177-1189.

Holton, J. R., P. H. Haynes, M. E. McIntyre, A. R. Douglass, R. B. Rood, and L. Pfister (1995), Stratosphere-troposphere exchange. *Rev. Geophys.*, *33*, 403-439.

Jacoby, G. C., K. W. Workman, and R. D. D'Arrigo (1999), Laki eruption of 1783, tree rings, and disaster for northwest Alaska Inuit, *Quat. Sci. Rev.*, *18*, 1365-1371.

Jöckel, P., C. A. M. Brenninkmeijer, and P. J. Crutzen (2003), A discussion on the determination of atmospheric OH and its trends, *Atmos. Chem. Phys.*, *3*, 107–118.

Kirchner, I., G. L. Stenchikov, H.-F. Graf, A. Robock and J. C. Antuña (1999), Climate model simulation of winter warming and summer cooling following the 1991 Mount Pinatubo volcanic eruption, *J. Geophys. Res.*, *104*, 19,039-19,055.

Koch, D., D. Jacob, I. Tegen, D. Rind, and M. Chin (1999), Tropospheric sulfur simulation and sulfate direct radiative forcing in the Goddard Institute for Space Studies general circulation model, *J. Geophys. Res.*, *104*, 23,799-23,822.

Koch, D., G. A. Schmidt, and C. Field (2006), Sulfur, sea salt and radionuclide aerosols in GISS ModelE, *J. Geophys. Res.*, in press.

Lacis, A. A., and V. Oinas (1991), A description of the correlated k-distribution method for modeling nongray gaseous absorption, thermal emission, and multiple scattering in vertically inhomogeneous atmospheres, *J. Geophys. Res.*, *96*, 9027-9063.

Lamb, H. H. (1970), Volcanic dust in the atmosphere; with a chronology and assessment of its meteorological significance. *Phil, Trans. R. Soc. (London)*, *266*, 425-533.

Lambert, A., R. G. Grainger, J. J. Remedios, C. D. Rogers, M. Corney, and F. W. Taylor (1993), Measurements of the evolution of the Mt. Pinatubo aerosol cloud by ISAMS, *Geophys. Res. Lett.*, *20*, 1287-1290.

Legrand, M. R., and R. J. Delmas (1988), Formation of HCl in the Antarctic atmosphere, *J. Geophys. Res.*, *93*, 7,153-7,168.

Long, C. S., and L. L. Stowe (1994), Using the NOAA/AVHRR to study stratospheric aerosol optical thickness following the Mt. Pinatubo eruption, *Geophys. Res. Lett.*, *21*, 2215-2218.

Mosley-Thompson, E., T. A. Mashiotta, and L. G. Thompson (2003), High resolution ice core records of late Holocene volcanism: Current and future contributions from the Greenland PARCA cores, in *Volcanism and the Earth's Atmosphere*, edited by A. Robock and C. Oppenheimer, pp. 153-164, AGU, Washington, D.C.

Oman, L., A. Robock, G. Stenchikov, G. A. Schmidt, and R. Ruedy (2005), Climatic response to high-latitude volcanic eruptions, *J. Geophys. Res.*, *110*, D13103, doi:10.1029/ 2004JD005487.

Palais, J., and H. Sigurdsson (1989), Petrologic evidence of volatile emissions from major historic and prehistoric volcanic eruptions, in *Understanding Climate Change*, Geophys. Monogr. Ser., vol. 52, edited by A. Berger, pp. 31–53, AGU, Washington, D. C.

Pinto, J. P., R. P. Turco, and O. B. Toon (1989), Self-Limiting Physical and Chemical Effects in Volcanic Eruption Clouds, *J. Geophys. Res.*, *94*, 11,165-11,174.

Ramachandran, S., V. Ramaswamy, G. L. Stenchikov, and A. Robock (2000), Radiative impacts of the Mt. Pinatubo volcanic eruption: Lower stratospheric response, *J. Geophys. Res.*, *105*, 24,409-24,429.

Read, W. G., L. Froidevaux, and J. W. Waters (1993), Microwave Limb Sounder measurements of stratospheric SO_2 from the Mt. Pinatubo volcano, *Geophys. Res. Lett.*, *20*, 1299-1302.

Robock, A. (2000), Volcanic eruptions and climate, *Rev. Geophys.*, *38*, 191-219.

Russell, P. B., et al. (1996), Global to microscale evolution of the Pinatubo volcanic aerosol derived from diverse measurements and analyses, *J. Geophys. Res. 101*, 18,745-18,763.

Sato, M., J. E. Hansen, M. P. McCormick, and J. B. Pollack (1993), Stratospheric aerosol optical depths, 1850-1990, *J. Geophys. Res.*, *98*, 22,987-22,994.

Schmidt, G. A., et al. (2006), Present day atmospheric simulations using GISS ModelE: Comparison to in-situ, satellite and reanalysis data, *J. Clim.*, *19*, 153-192.

Stenchikov, G. L., I. Kirchner, A. Robock, H.-F. Graf, J. C. Antuña, R. G. Grainger, A. Lambert, and L. Thomason (1998), Radiative forcing from the 1991 Mount Pinatubo volcanic eruption, *J. Geophys. Res.*, *103*, 13,837-13,857.

Stevenson, D. S., C. E. Johnson, E. J. Highwood, V. Gauci, W. J. Collins, and R. G. Derwent (2003), Atmospheric impact of the 1783-1784 Laki eruption: Part I chemistry modelling, *Atmos. Chem. Phys., 3*, 487-507.

Stothers, R. B. (1996a), Major optical depth perturbations to the stratosphere from volcanic eruptions: Pyrheliometric period, 1881-1960, *J. Geophys. Res.*, *101*, 3901-3920.

Stothers, R. B. (1996b), The Great Dry Fog of 1783, *Climatic Change*, *32*, 79-89.

Stothers, R. B. (1997), Stratospheric aerosol clouds due to very large volcanic eruptions of the early twentieth century: Effective particle sizes and conversion from pyrheliometric to visual optical depth, *J. Geophys. Res.*, *102*, 6143-6151.

Stothers, R. B. (2001), A chronology of annual mean effective radii of stratospheric aerosols from volcanic eruptions during the twentieth century as derived from ground-based spectral extinction measurements, *J. Geophys. Res.*, *106*, 32,043-32,049.

Tang, I. N. (1996), Chemical and size effects of hygroscopic aerosols on light scattering coefficients, *J. Geophys. Res.*, *101*, 19,245-19,250.

Thomason, L. W., L. R. Poole, and T. Deshler (1997), A global climatology of stratospheric aerosol surface area density deduced from Stratospheric Aerosol and Gas Experiment II measurements: 1984-1994, *J. Geophys. Res.*, *102*, 8,967-8,976.

Thordarson, T., and S. Self, (1993), The Laki (Skaftár Fires) and Grímsvötn eruptions in 1783-1785, *Bull. Volc.*, *55*, 233-263.

Thordarson, T., S. Self, N. Óskarsson, and T. Hulsebosch, 1996. Sulfur, chlorine and fluorine degassing and atmospheric loading by the 1783-1784 AD Laki (Skaftár Fires) eruption in Iceland, *Bull. Volc.*, *58*, 205-225.

Thordarson, T. and S. Self (2003), Atmospheric and environmental effects of the 1783-1784 Laki eruption: A review and reassessment, *J. Geophys. Res.*, *108* (D1), 4011, doi:10.1029/2001JD002042.

Timmreck, C., H.-F. Graf, and I. Kirchner (1999), A one and half year interactive MA/ECHAM4 simulation of Mount Pinatubo Aerosol, *J. Geophys. Res.*, *104*, 9,337-9,359.

Trepte, C. R., and M. H. Hitchman (1992), Tropical stratospheric circulation deduced from satellite aerosol data, *Nature*, *335*, 626-628.

Zielinski, G. A. (1995), Stratospheric loading and optical depth estimates of explosive volcanism over the last 2100 years derived from the Greenland Ice Sheet Project 2 ice core, *J. Geophys. Res.*, *100*, 20,937–20,955.

Table 1. Total sulfate aerosol yield of the 1783-1784 Laki eruption determined with different methods.

Study	Mass (Mt)	Method
Clausen and Hammer [1988]	374	Ice cores
Zielinski [1995]	46-59	Ice cores
Stothers [1996]	200	Radiation
Clausen et al. [1997]	138-210	Ice cores
Thordarson and Self [2003]	200	Geology
Stevenson et al. [2003]	71-92	Aerosol model
This study	163-166	Aerosol model

FIGURE CAPTIONS

Figure 1. Daily mass of SO_2 gas (Mt) for Laki eruption used in modelE runs from 1 June 1783 to 7 February 1784, based on Figure 2 from *Thordarson and Self* [2003]. The lower troposphere (LT) injection is shown in green and the upper troposphere/lower stratosphere (UT/LS) is shown in blue.

Figure 2. Daily mass loading of SO_2 and SO_4 (Mt) for the three simulations of Pinatubo (left) and Katmai (right) with the background loadings removed. The Pinatubo simulations are from May 1991 through August 1993. The Katmai simulations are from May 1912 through August 1914.

Figure 3. Zonal mean sulfate optical depth for Pinatubo from three modelE simulation, compared to SAGE II, and AVHRR data with backgrounds removed. The bottom panel is global average optical depth for the three individual modelE runs, SAGE II and AVHRR. The optical depths are from May 1991 through August 1993.

Figure 4. Zonal mean sulfate optical depth for Katmai from three modelE simulation, compared to *Ammann et al*. [2003], and *Sato et al.* [1993] data with backgrounds removed. The bottom panel is Northern Hemisphere average optical depth for the three individual modelE runs, *Ammann et al*. [2003], and *Sato et al.* [1993]. The optical depths are from May 1912 through August 1914.

Figure 5. Daily mass loading of SO_2 and SO_4 (Mt) for the three simulation of the Laki eruption with the background loadings removed. The Laki simulations are from May 1783 through August 1785.

Figure 6. Zonal mean sulfate optical depth for Laki from three modelE simulation with backgrounds removed. The bottom panel is Northern Hemisphere average optical depth for

the three individual modelE runs. The optical depths are from May 1783 through August 1785.

Figure 7. (a) Total SO_4 (kg/km^2) deposition from the Laki eruption to Greenland and surrounding areas averaged from the 3 simulations. The 2000 m elevation is shown on Greenland. (b) Total SO_4 (kg/km^2) deposition from 23 Greenland ice cores [*Gao et al.*, manuscript in preparation].

Figure 8. The 30°W-45°E mean SO_2 (left) and SO_4 (right) concentrations (ppbv) for June-August 1783 over the Northern Hemisphere from the surface to 30 mb.

Figure 9. Zonal mean SO_4 concentrations (ppbv) for the Laki eruption over the Northern Hemisphere from May 1783 through January 1785 for 171 mb (top), 280 mb (center), and 945 mb (bottom).

Figure 10. All-sky radiative forcings (W/m^2) calculated for the Laki eruption from January 1783 through December 1784 for the Northern Hemisphere. Shown on the left are TOA shortwave forcing (a) and TOA longwave forcing (b), as well as the TOA net radiative forcing (c). Shown on the right are surface shortwave forcing (d) and surface longwave forcing (e), as well as the surface net radiative forcing (f).

Figure 11. Zonal mean monthly averaged heating rate anomalies (K/day) for August 1783 (left column) and January 1784 (right column) from the surface to 1 mb for the Northern Hemisphere. Shown are shortwave heating rate anomalies (a and d), longwave heating rate anomalies (b and d), and total heating rate anomalies (c and f).

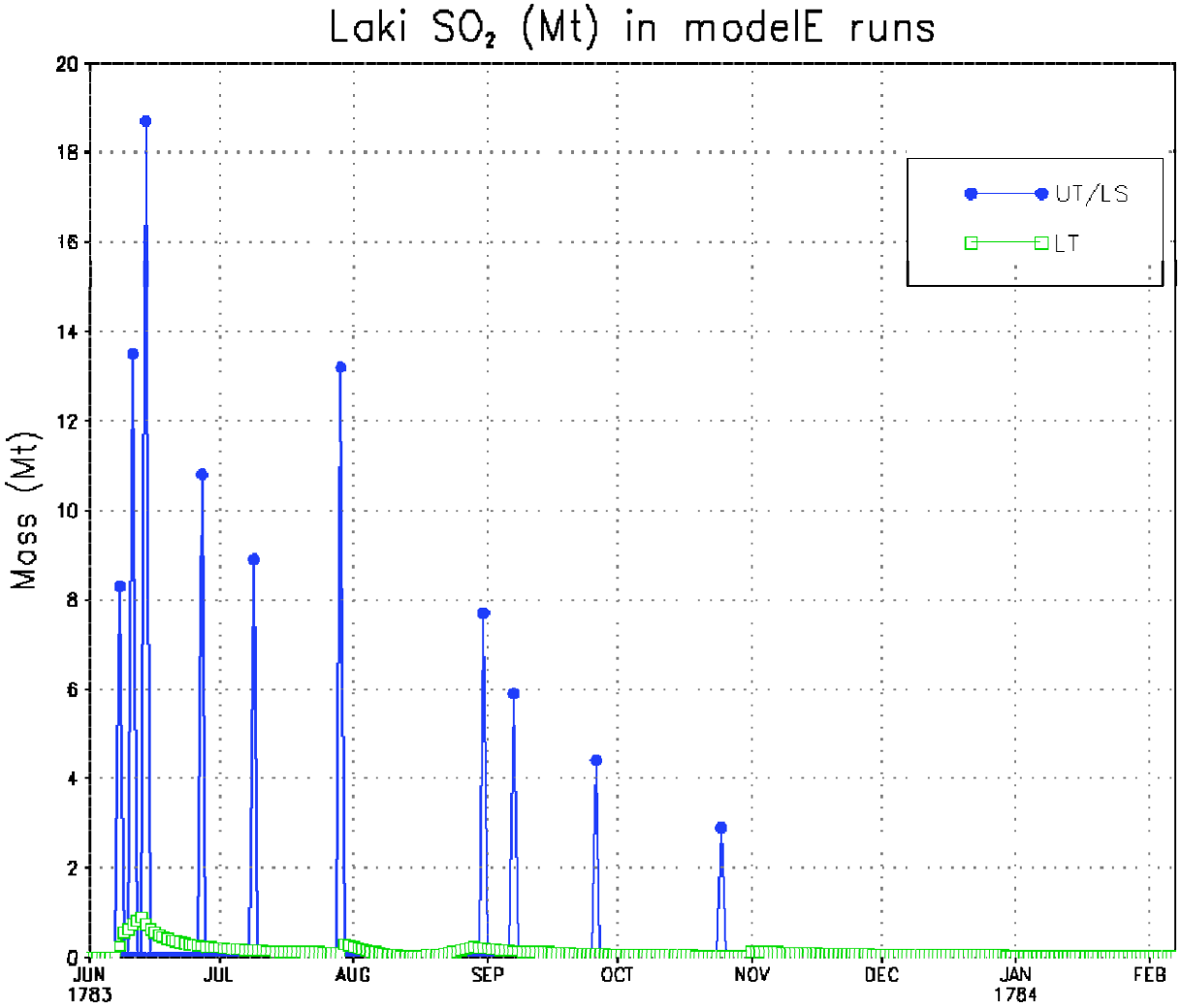

Figure 1. Daily mass of SO_2 gas (Mt) for Laki eruption used in modelE runs from 1 June 1783 to 7 February 1784, based on Figure 2 from *Thordarson and Self* [2003]. The lower troposphere (LT) injection is shown in green and the upper troposphere/lower stratosphere (UT/LS) is shown in blue.

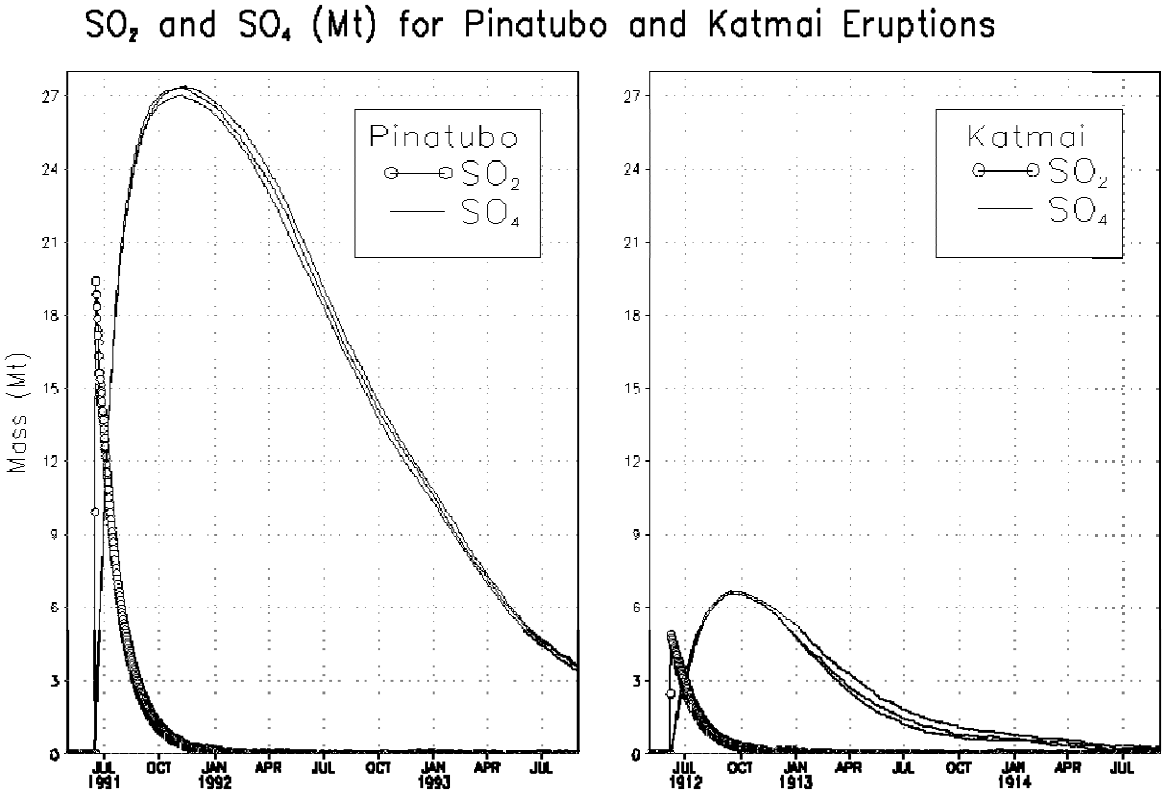

Figure 2. Daily mass loading of SO_2 and SO_4 (Mt) for the three simulations of Pinatubo (left) and Katmai (right) with the background loadings removed. The Pinatubo simulations are from May 1991 through August 1993. The Katmai simulations are from May 1912 through August 1914.

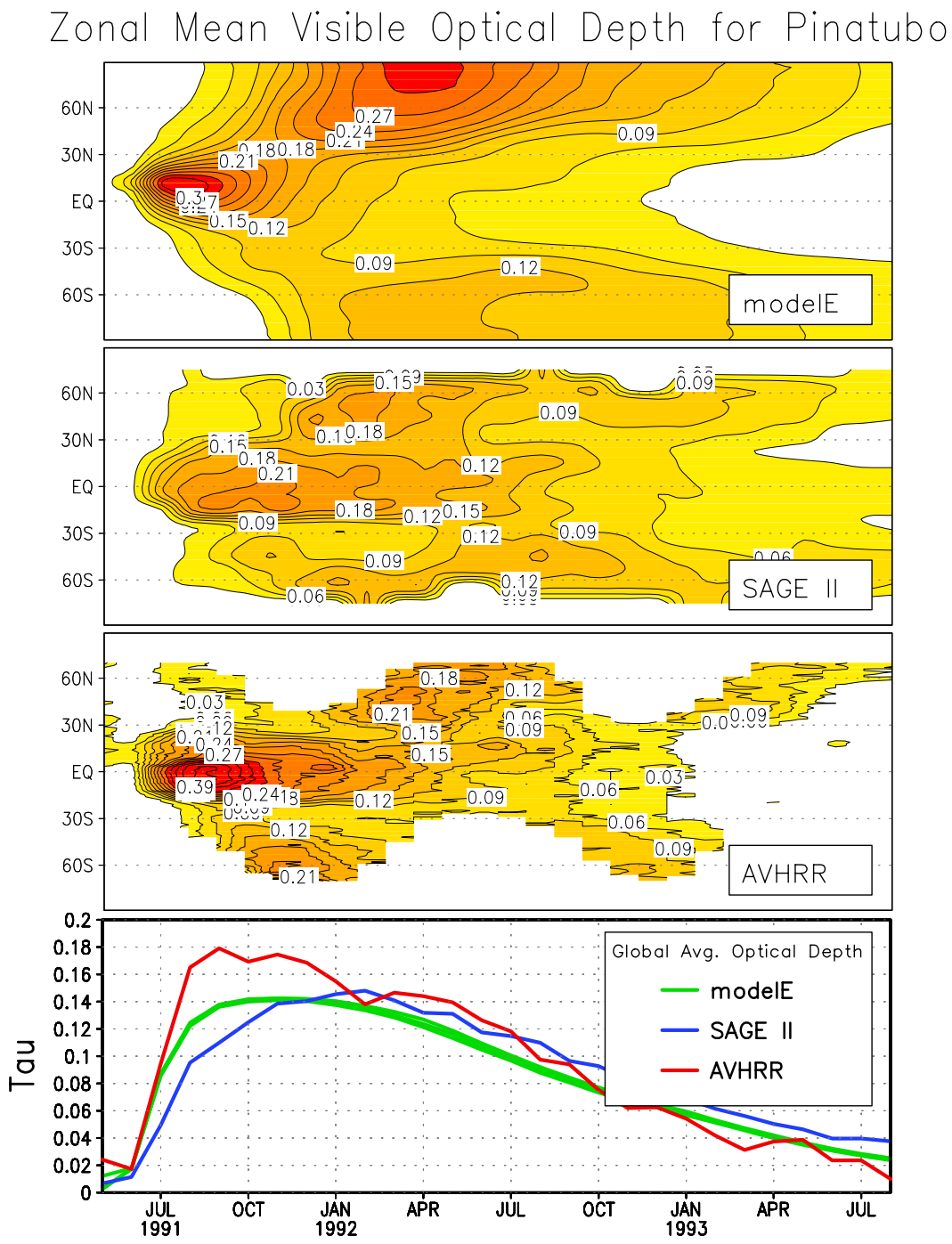

Figure 3. Zonal mean sulfate optical depth for Pinatubo from 3 modelE simulation, compared to SAGE II, and AVHRR data with backgrounds removed. The bottom panel is global average optical depth for the 3 individual modelE runs, SAGE II and AVHRR. The optical depths are from May 1991 through August 1993.

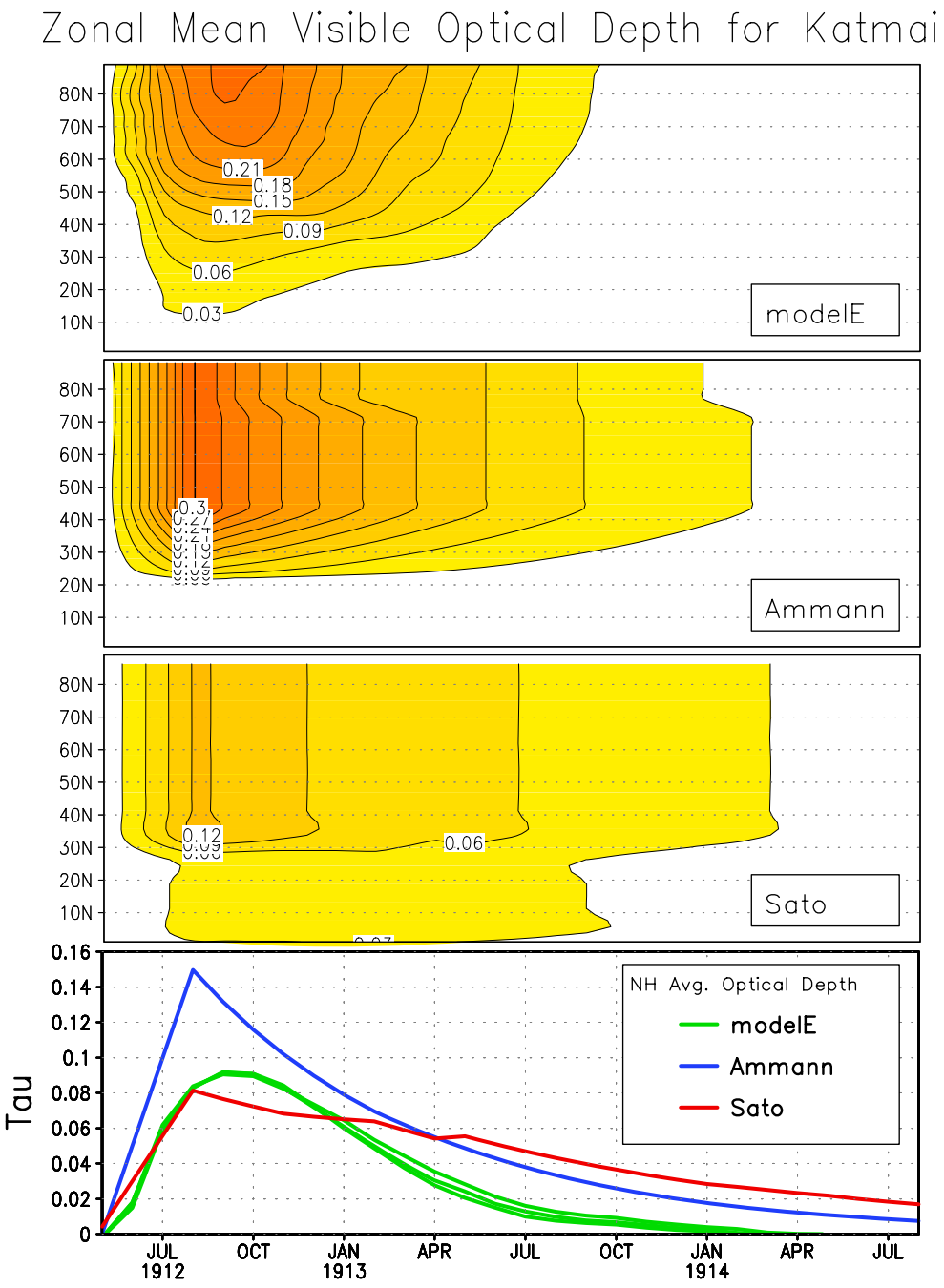

Figure 4. Zonal mean sulfate optical depth for Katmai from 3 modelE simulation, compared to *Ammann et al*. [2003], and *Sato et al.* [1993] data with backgrounds removed. The bottom panel is Northern Hemisphere average optical depth for the 3 individual modelE runs, *Ammann et al*. [2003], and *Sato et al.* [1993]. The optical depths are from May 1912 through August 1914.

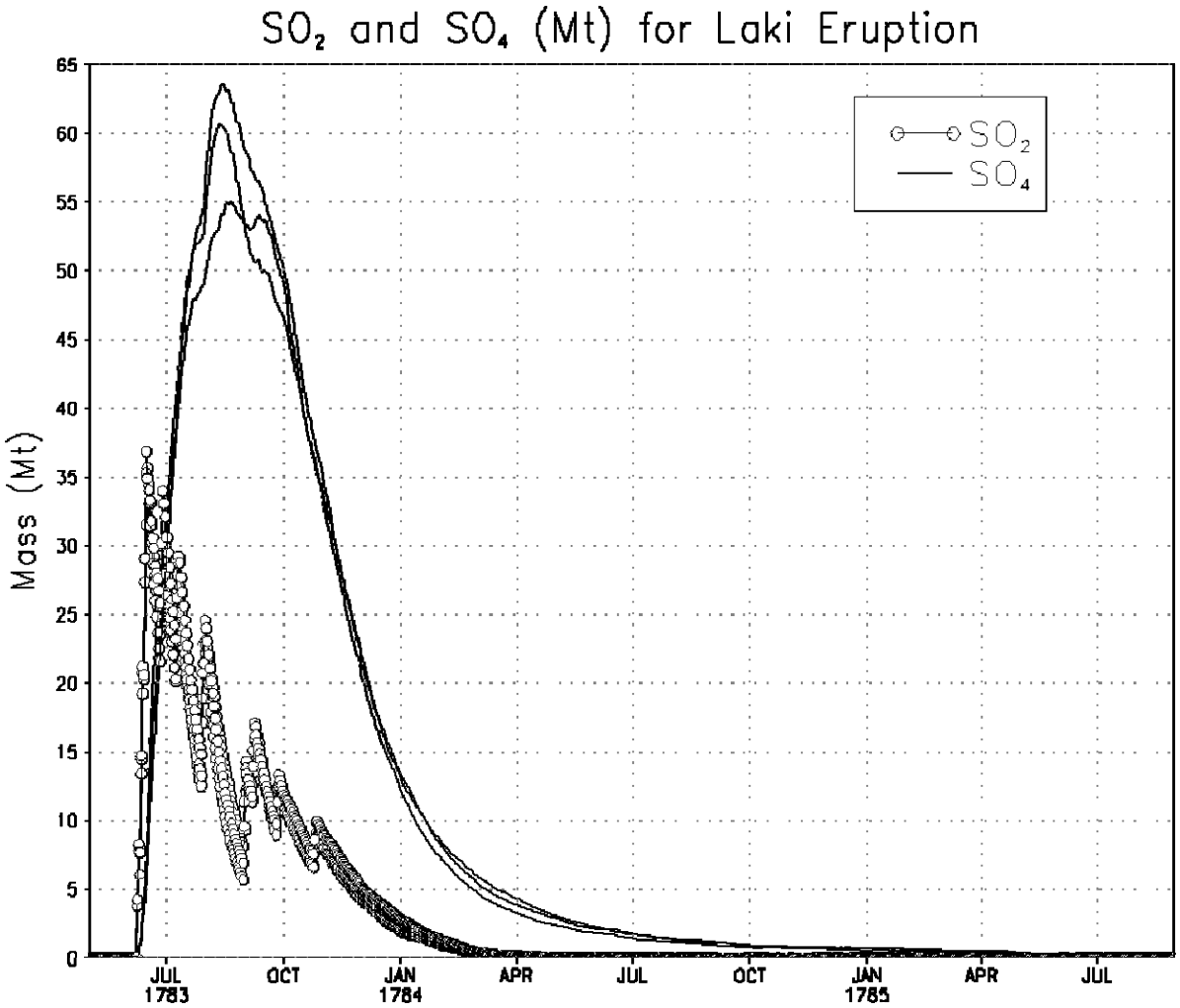

Figure 5. Daily mass loading of SO_2 and SO_4 (Mt) for the 3 simulation of the Laki eruption with the background loadings removed. The Laki simulations are from May 1783 through August 1785.

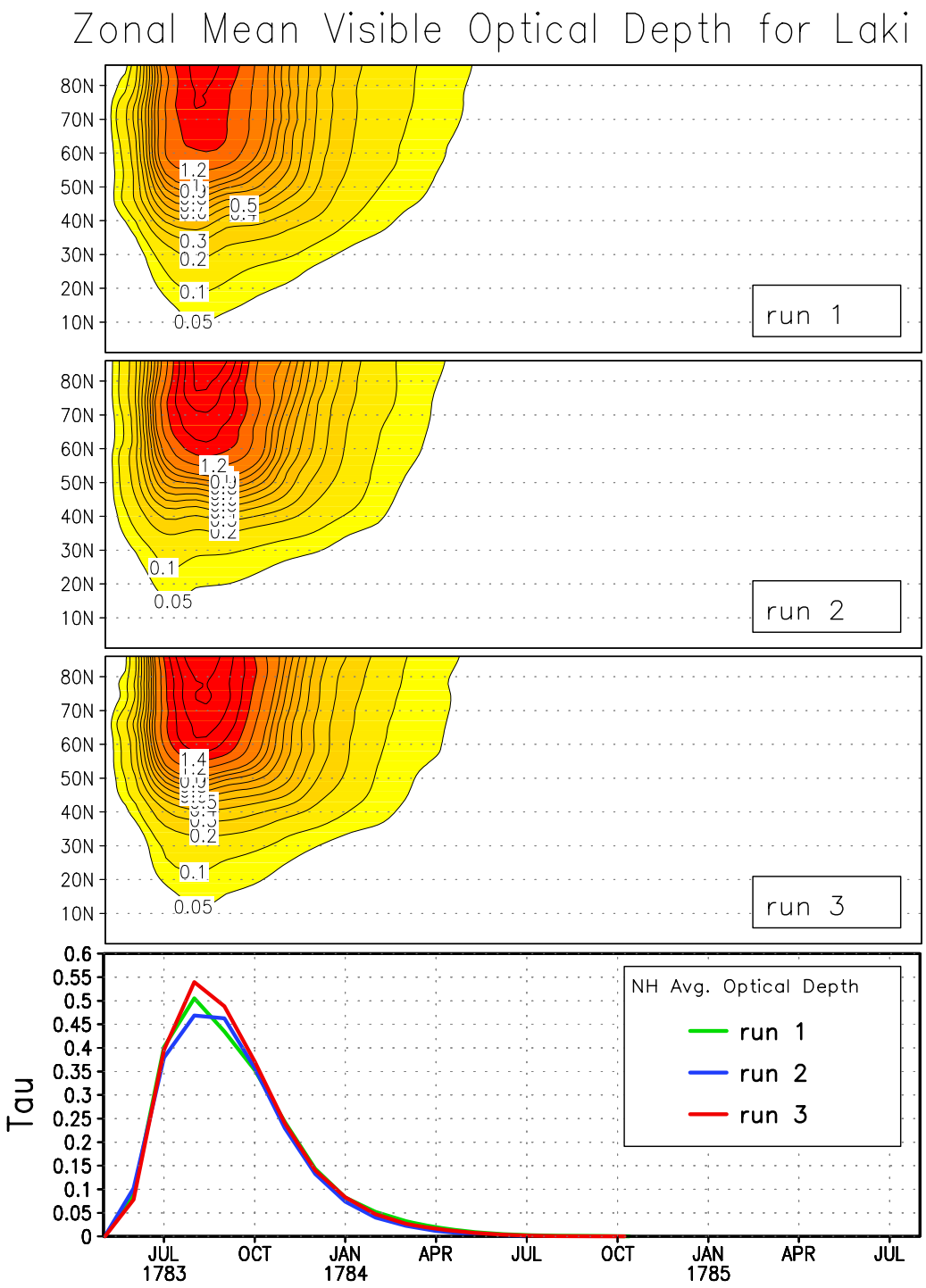

Figure 6. Zonal mean sulfate optical depth for Laki from 3 modelE simulation with backgrounds removed. The bottom panel is Northern Hemisphere average optical depth for the 3 individual modelE runs. The optical depths are from May 1783 through August 1785.

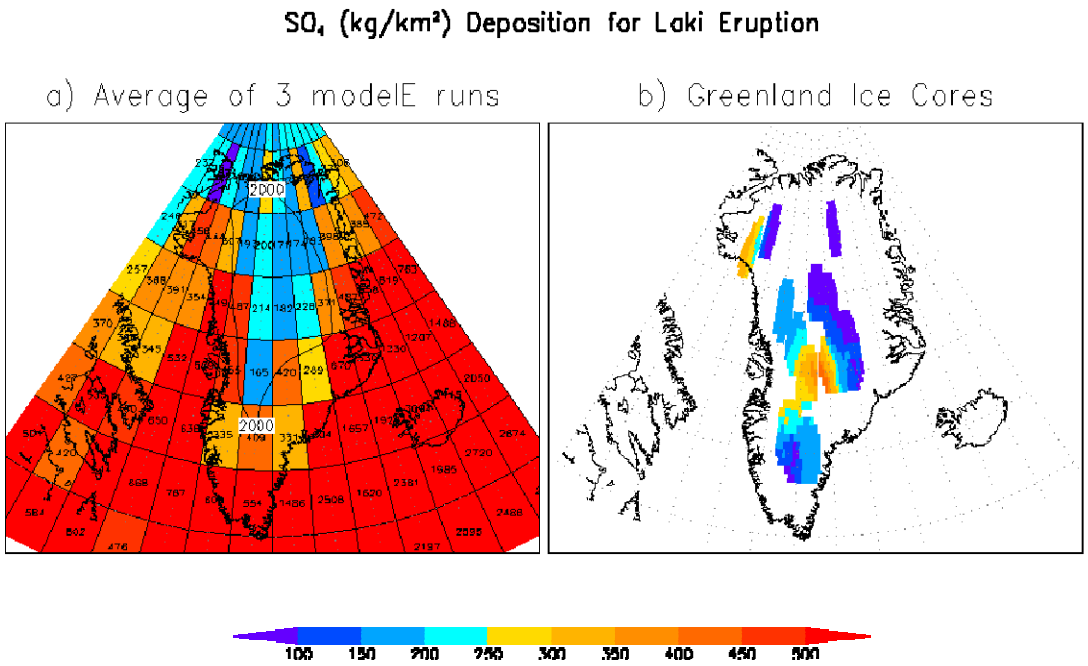

Figure 7. (a) Total SO_4 (kg/km^2) deposition from the Laki eruption to Greenland and surrounding areas averaged from the 3 simulations. The 2000 m elevation is shown on Greenland. (b) Total SO_4 (kg/km^2) deposition from 23 Greenland ice cores [*Gao et al.*, manuscript in preparation].

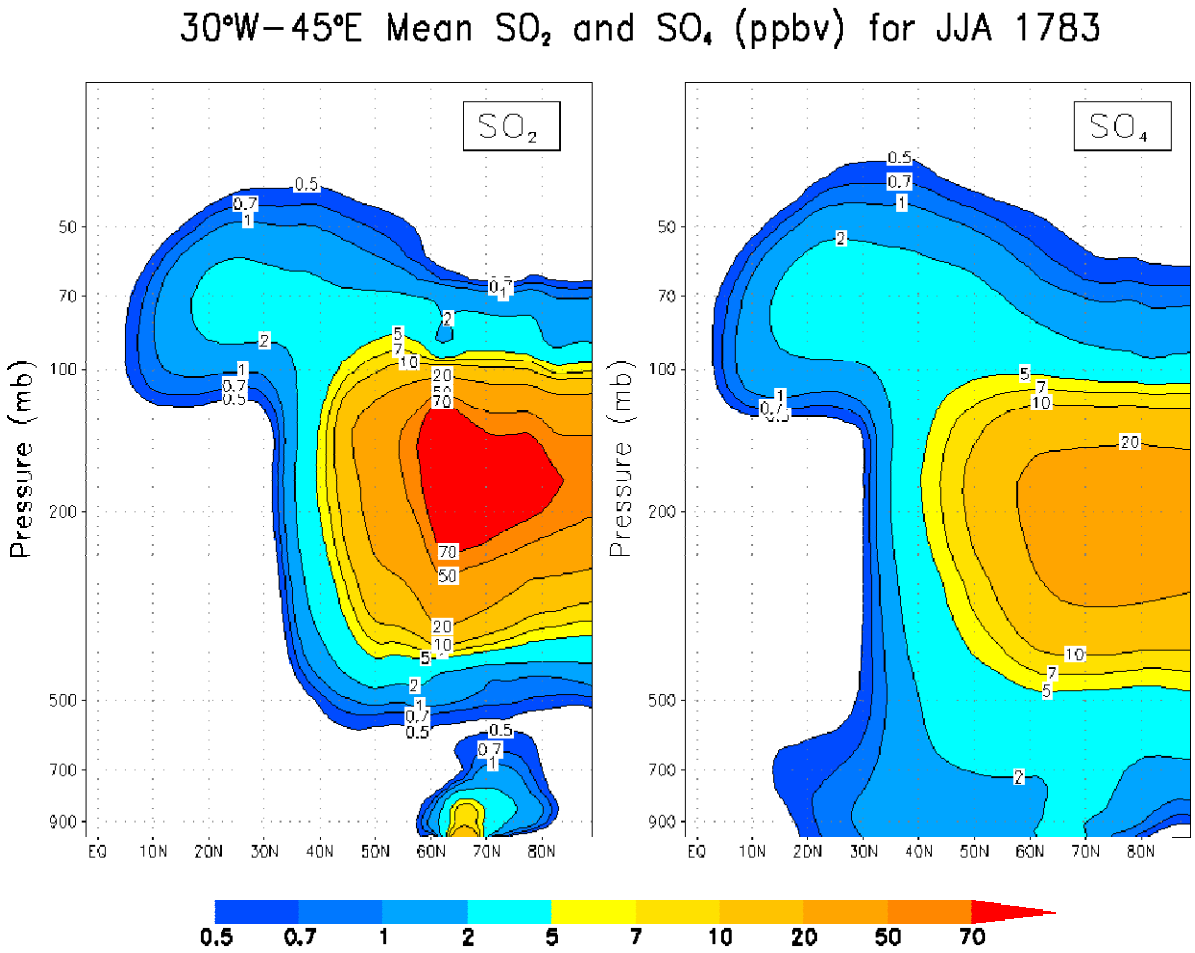

Figure 8. The 30°W-45°E mean SO_2 (left) and SO_4 (right) concentrations (ppbv) for June-August 1783 over the Northern Hemisphere from the surface to 30 mb.

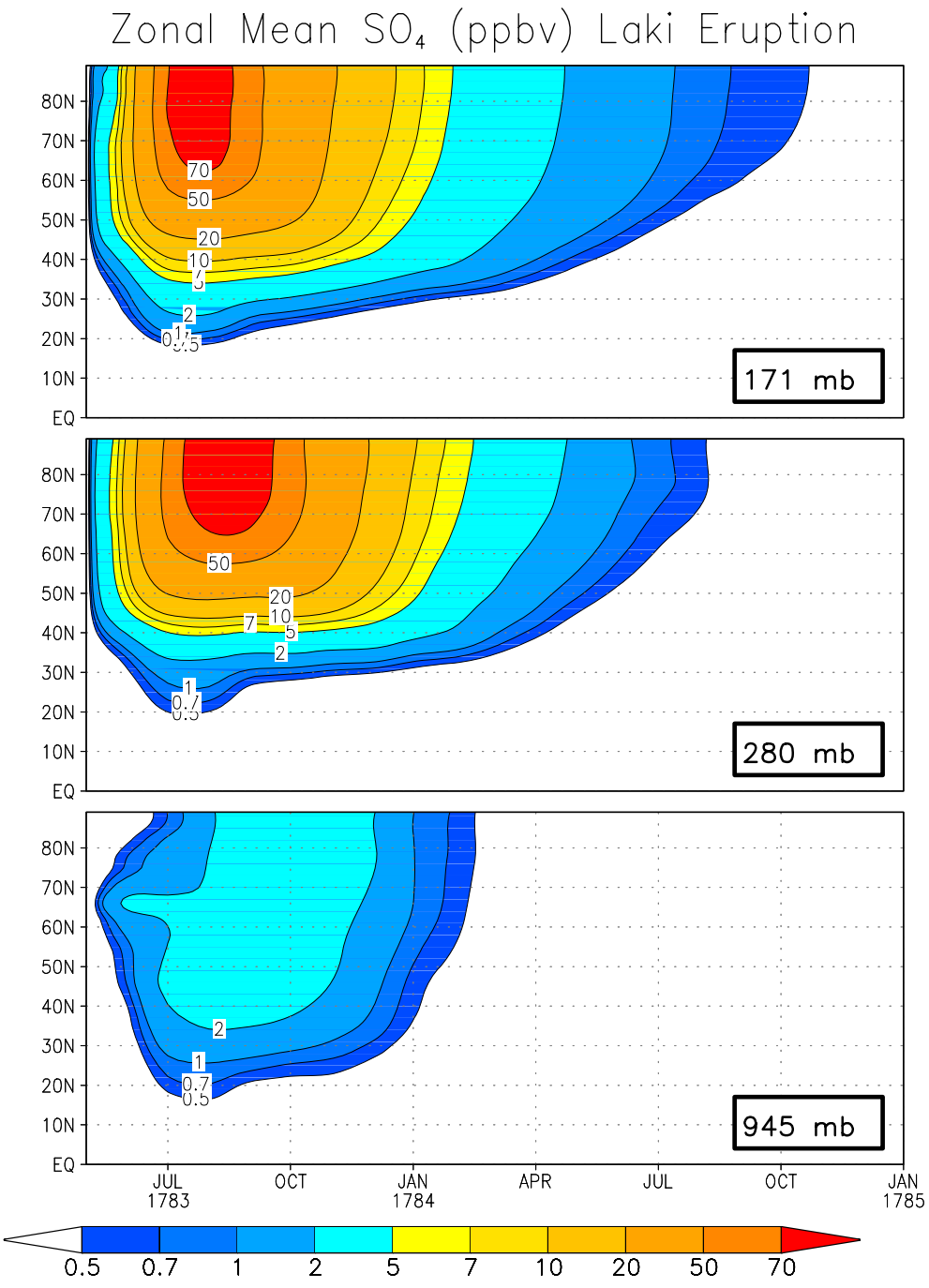

Figure 9. Zonal mean SO_4 concentrations (ppbv) for the Laki eruption over the Northern Hemisphere from May 1783 through January 1785 for 171 mb (top), 280 mb (center), and 945 mb (bottom).

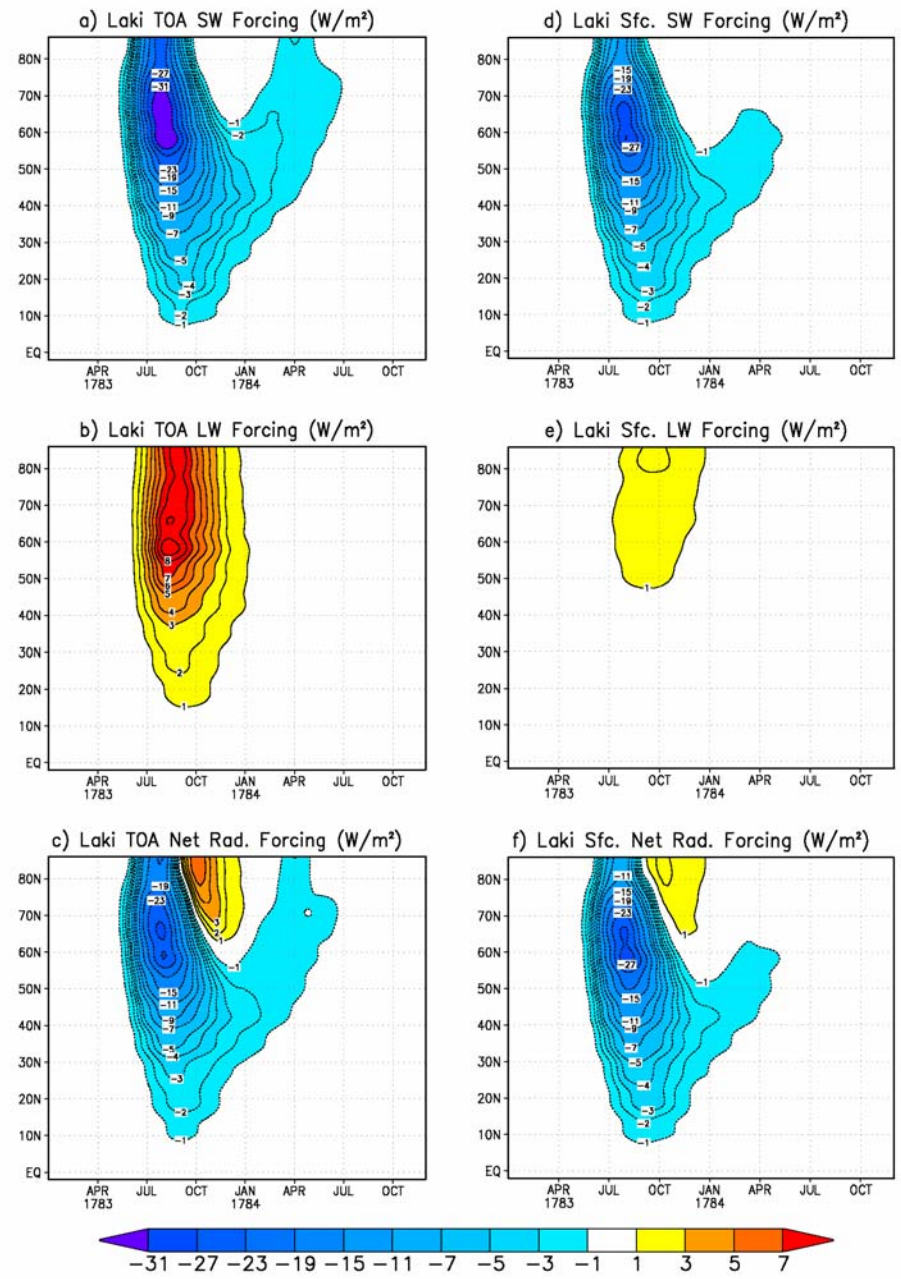

Figure 10. All-sky radiative forcings (W/m^2) calculated for the Laki eruption from January 1783 through December 1784 for the Northern Hemisphere. Shown on the left are TOA shortwave forcing (a) and TOA longwave forcing (b), as well as the TOA net radiative forcing (c). Shown on the right are surface shortwave forcing (d) and surface longwave forcing (e), as well as the surface net radiative forcing (f).

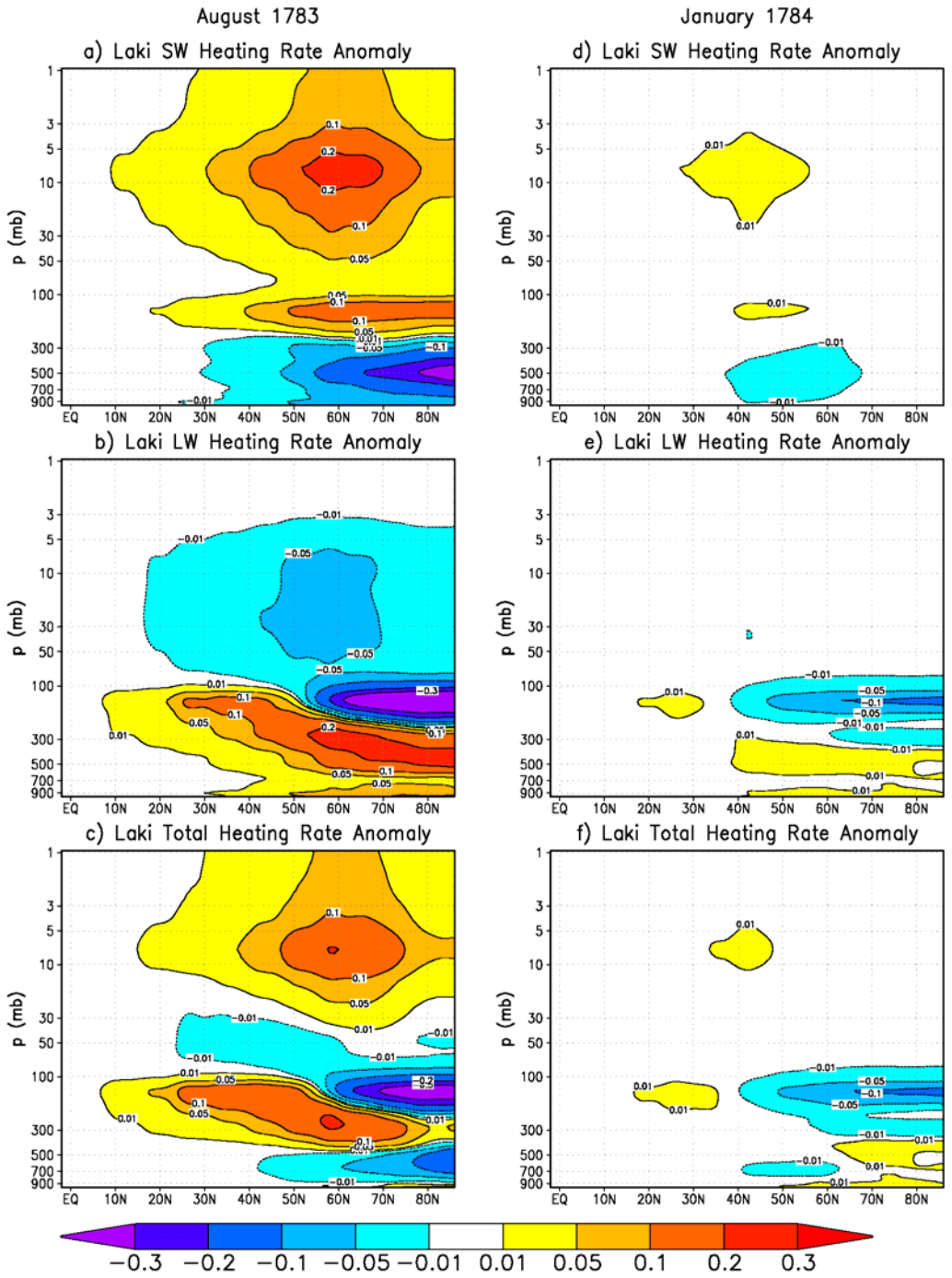

Figure 11. Zonal mean monthly averaged heating rate anomalies (K/day) for August 1783 (left column) and January 1784 (right column) from the surface to 1 mb for the Northern Hemisphere. Shown are shortwave heating rate anomalies (a and d), longwave heating rate anomalies (b and d), and total heating rate anomalies (c and f).